Hydrogen-bond networks in linear, branched and tertiary alcohols

S.K. Stephenson[a,*], R.D. Offeman[b], G.H. Robertson[b], W.J. Orts[b]

[a]*Dow Chemical Company, Freeport, TX 77541, USA*
[b]*Western Regional Research Center, Agricultural Research Service, US Department of Agriculture, Albany, CA 94710, USA*

Abstract

Molecular dynamics simulations are used to determine the hydrogen-bond networks formed by 54 linear and branched alcohols containing 5–20 carbon atoms, and the results show systematic differences in their hydrogen-bonded structures, depending both on hydroxyl group position and the alcohol's molecular weight. The hydrogen-bonded networks within these pure solvents correspond with experimentally determined water capacities for solvents in four main structural classes. These categories are: primary alcohols, secondary alcohols, tertiary alcohols, and alcohols with the branching point removed from the hydroxyl group. Each of these structural classes exhibits unique behavior in the correlation between the extended hydrogen-bond networks and observed capacities for water.
© 2007 Elsevier Ltd. All rights reserved.

Keywords: Extraction; Solvent effects; Hydrogen-bonded liquids; Molecular dynamics; Separations

1. Introduction

Solubilities of organic molecules, liquid–liquid equilibria and solvent extraction have long been of interest both from the perspective of fundamental chemical interactions and from that of the chemical process engineer. Studies on hydrogen-bonding and the intermolecular interactions within bulk water and small alcohols, as well as mixtures thereof, have recently been performed using both molecular simulation (González et al., 2004; Laaksonen et al., 1997; Padró et al., 1997) and neutron scattering techniques (Bakó et al., 2000; Bowron et al., 1998; Bowron and Moreno, 2002, 2003; Dixit et al., 2002). The fundamental understanding of intermolecular interactions within a given solvent can aid in making choices regarding solvent use for engineering-type applications. Although this understanding is actively being developed for small alcohols ($\leqslant 4$ carbons), the extension must be made to larger alcohols as well as to other solvents. Recently, molecular dynamics results for linear alcohols from C5–C12 were presented by Stephenson et al. (2006) showing intriguing trends in the intermolecular interaction with

the series. From these recent results the hypothesis that the hydrogen-bonding within linear alcohols affects their extraction properties in a systematic way is supported. Here, molecular dynamics studies of neat alcohols are extended to include 32 linear, branched and tertiary alcohols with the purpose of understanding what, if any, correlation can be made between the hydrogen-bonding of a neat alcohol and its capacity for ethanol or water. Such a trend would enable the prediction of ethanol and water capacities in liquid–liquid extractions (LLEs) by calculational methods. The focus here is primarily on the molecular dynamics experiments and resulting data. However, comparisons of these results with previously reported laboratory results for ethanol extraction by these same alcohols will be presented and discussed.

Since one of the ultimate goals of these molecular dynamics studies is to be able to predict LLE properties by calculating fundamental interactions within a solvent, it is useful to briefly explain the interest in extraction. LLE has long been explored as a possible low energy method of removing products from fermentation broths (Daugulis et al., 1991; Maiorella et al., 1984; Othmer and Ratcliffe, 1943). With the increasing importance of the biorefinery as a source of renewable fuels and chemical feedstocks (Kim and Dale, 2004), there is particular interest in the development of less-energy intensive

---

alternatives to distillation for the separation process (Lynd et al., 1999; Wyman, 2003). An especially large impact of using less-energy intensive methods could be seen in the overall energy balance and profitability of fuel ethanol production (Madson and Monceaux, 1999).

As mentioned earlier, the ultimate goal is to develop a method of predicting the capacities of a given solvent for ethanol and water based on hydrogen-bonding patterns in the neat solvent as observed by molecular dynamics simulations. Since a solvent's capacity for either water or ethanol must be governed by a combination of hydrophilic and hydrophobic interactions, it is logical that a solvent's interaction with itself can act as a good indicator for the other capacities. Previous attempts to predict extraction performance for solvents have included cone-angle and steric-hinderance arguments based on the structure of a single alcohol molecule (Munson and King, 1984; Offeman et al., 2005b), empirical thermodynamic group contribution models (Fredenslund et al., 1975; Magnussen et al., 1981; Wu and Sandler, 1991), and conductor-like screening model for realistic solvation (COSMO-RS) which is a continuum solvation model based on quantum chemical calculations (Eckert and Klamt, 2002; Klamt, 2005).

The cone-angle and steric-hinderance approaches presented by Munson and King (1984) deal exclusively with the structure of a single molecule and the possible conformations that might block, or shield, the hydroxyl group. However, this does not account for the intermolecular interactions occurring in alcohols and other hydrogen-bonded or polar solvents.

The most commonly used predictive techniques have been thermodynamic group contribution methods, as reviewed by Poling et al. (2001) and Prausnitz and Tavares (2004). These models treat solvent molecules as series of groups, each contributing to the overall properties of the solvent. The most prevalent of these models is the UNIFAC model, which in its initial form did not account for positional information of the groups (Fredenslund et al., 1975). Later extensions added positional information to the UNIFAC model, but the accuracy for predicting the extractive performance of isomers could still use improvement (Chen and Mathias, 2002). The popularity of the UNIFAC model is due to its speed and ease of use. However, it does not provide a physical description of the balance between hydrophobic and hydrophilic interactions within solvents, nor does it lead to a molecular level understanding of the extraction process.

A recent, and very intriguing, development toward predicting LLE data is the COSMO-RS, a quantum mechanical approach (Eckert and Klamt, 2002; Klamt, 2005). This is an extension of a dielectric continuum solvation method based on quantum chemical calculations. COSMO-RS computes a molecular surface polarization charge density (σ) distribution for a given solvent and accounts for electrostatic misfit and hydrogen-bond contributions. The thermodynamics of solvent mixtures, or solute/solvent combinations, can then be described by comparisons of the individual σ-profiles. COSMO-RS has been used to predict activity coefficients and has been applied to solvent selection problems (Klamt, 2005). Its success is through a thermodynamic description of solvent–solvent and solvent–solute

interactions. This can lead to quantitative prediction of ternary liquid–liquid equilibrium tie-line data for a given system, but it does not provide a physical picture of molecular-level interactions and orientations of the solvent.

Still, the most accurate method of determining which solvents are the best extractants of ethanol from water is to screen them experimentally. Several recent articles present LLE results from series of alcohols, oils, oil derivatives and esters (Offeman et al., 2005b, 2006). The alcohols screened have 5–20 carbon atoms (C5–C20) with varieties of carbon branching patterns and hydroxyl group locations. Many trends in the extraction results have been discussed dealing with characteristics of individual solvent molecules such as molecular weight, hydroxyl group position and branching patterns. However, a thorough molecular picture, including hydrophilic and hydrophobic intermolecular interactions within the solvent, is still being developed. A first step toward this, presented recently by Stephenson et al. (2006), noted a trend between molecular dynamics simulations for purely linear alcohols and observed capacities for water and ethanol. It was shown that the hydrogen-bonded network in a given solvent correlates well to the experimentally observed capacities for water; whereas, the solvent's capacity for ethanol is mostly dependent on solvent hydroxyl group concentration, a function of 1000/molecular weight.

Here, the molecular dynamics simulation work is extended to include small-branched alcohols ($\leqslant$C12), as well as the larger (C16–C20) β-branched alcohols for which extraction data was recently obtained Stephenson et al. (2006). The alcohols studied here can be classified into four different groups based on structure: unbranched primary alcohols (UP), branched primary alcohols (BP), secondary alcohols (S) and tertiary alcohols (T). Each of these classes has different trends in the correlation between the hydrogen-bond network and the corresponding K_{DW} values. The results presented here provide insights into the effects of branching location and patterns on the bulk liquid structure of the various neat alcohols, although they do not quantitatively predict LLE data.

2. Theory and methods

2.1. Liquid–liquid extraction

LLE performances for various solvents can be compared by equilibrium distribution coefficients of the solute being extracted at a given set of operation conditions (i.e., temperature and initial aqueous phase ethanol concentration). In the case of solvent extraction of ethanol from aqueous solutions these are defined as

$$K_{DE} = [\text{EtOH}]_{\text{org}}/[\text{EtOH}]_{\text{aq}} \tag{1}$$

and

$$K_{DW} = [\text{H}_2\text{O}]_{\text{org}}/[\text{H}_2\text{O}]_{\text{aq}}, \tag{2}$$

for ethanol and water, respectively (King, 1971). These distribution coefficients reflect the solvent's capacity for ethanol or water. Their ratio, K_{DE}/K_{DW}, is the separation factor (α),

which quantifies the solvent's selectivity for ethanol over water. A high K_{DE} and a high α (i.e., a low K_{DW}) are desirable, but usually the higher a solvent's K_{DE}, the higher it's K_{DW}.

The experimental LLE results used in the correlations presented here were achieved using the screening method described in detail by Offeman et al. (2005a), which included an in-depth evaluation of possible sources of variation in LLE data. Steps were taken to minimize these errors, and this method has now been used to screen a total of 74 alcohols, oils and esters (Offeman et al., 2005b, 2006).

2.2. Molecular dynamics simulations

MD simulations were performed using the TINKER software package (Ponder, 2004) with the optimized potential for liquid simulation-united atom (OPLS-UA) forcefield (Jorgensen, 1986) on periodic boxes containing 200 solvent molecules. The OPLS-UA forcefield is a Lennard-Jones (12-6) forcefield and is one of the standards in the field of molecular dynamics. The big advantage of an UA (united atom) over an AA (all atom) forcefield is the significantly decreased computation time required when the hydrogens is grouped with the carbon to which they are attached rather than each treated individually. The OPLS-UA forcefield parameters are specifically design for specific "groups" such as a sp3 hybridized carbon with attached to two hydrogen atoms and two other carbon atoms. Such a carbon has a different parameter set than a sp3 hybridized carbon attached to two carbon atoms, one hydrogen atom and one oxygen atom. Since each unique "type" of carbon has its own parameter set based on the other atoms bonded to it, there is a lot of flexibility for modeling alcohols with various branching patterns. Further detail about the particulars of the OPLS-UA forcefield and its parameters can be found in Jorgensen (1986). The OPLS-UA forcefield has been well tested for low molecular weight alcohols up to 1-octanol (Best et al., 1999; Debolt and Kollman, 1995; Jorgensen, 1986). Although it has been suggested that the OPLS-UA parameter set is not transferable to alcohols larger than propanol (Van Leeuwen, 1996), it has been applied to successfully calculate octanol/water partition coefficients and the thermodynamics of neat 1-octanol (Best et al., 1999) indicating that the OPLS-UA forcefield is indeed applicable to larger alcohols as well. In order to validated this assumption, comparisons of calculated to experimental densities were made. The discussions of these will follow shortly, but the conclusion is that the OPLS-UA forcefield seems to be a good choice. An intriguing alternative to OPLS-UA could be the TraPPE-UA alcohol force field developed by Chen et al. (2001), which is designed with the intention of modeling phase equilibria. Future work should include comparisons of the OPLS-UA and TraPPE-UA forcefields for these branched alcohol systems. This was not pursued in the current study because the OPLS-UA forcefield is more widely used and accepted.

All periodic boxes were generated with initial dimensions calculated from the solvent's known density. The periodic box used here is a cube surrounded by images of itself on every face, edge and vertex. Every time an atom exits on one side of

Table 1
Calculated solvent densities

Solvent	Known density	Calculated density (9 Å cutoff)	Calculated density (15 Å cutoff)
2-Methyl-1-butanol	0.819	0.805	0.832
2-Methyl-1-pentanol	0.824	0.819	0.844
3-Methyl-1-pentanol	0.823	0.817	0.844
4-Methyl-1-pentanol	0.813	0.819	0.843
2-Methyl-3-pentanol	0.825	0.814	0.840
4-Methyl-2-pentanol	0.807	0.817	0.842
2-Methyl-3-hexanol	0.821	0.818	0.844
3,3-Dimethyl-1-butanol	0.817	0.834	0.855
2,2-Dimethyl-3-pentanol	0.826	0.833	0.859
2,4-Dimethyl-3-pentanol	0.829	0.824	0.851
Iso-octadecanol (four terminal CH_3 groups)	0.847	0.867	0.884
2-Octyl-1-dodecanol	0.838	0.867	0.884

the box, it reenters from the other (Allen and Tildesley, 1987; Chandler, 1987). Molecular dynamics trajectories were calculated using the NPT ensemble at 298 K and 1 atm. Groningen-style pressure and temperature bath coupling constrained the conditions at STP (Berendsen, 1984), the RATTLE algorithm constrained bond distances, and the Ewald summation was used for the long-range electrostatic interactions (Allen and Tildesley, 1987).

The cutoff distance for non-bonded interactions was set at 9 Å, as justified by calculated solvent densities. Trajectories for several solvents were also calculated using a cutoff distance of 15 Å, but the resulting densities were significantly higher than those both from known STP densities and from the densities calculated at 9 Å. Table 1 compares known densities to those obtained from trajectories for 12 branched alcohols with molecular weights ranging from 88.15 to 298.55 g/mol. Densities reported are averages over the final 200 ps of the trajectory. Results using the shorter cutoff tend to match known densities within ±0.01 g/mL for the midsize alcohols (⩽C12), but the C18 and C20 alcohols have densities that are 0.02–0.03 g/mL high. In comparison, the densities calculated using the longer cutoff are considerably too high for all alcohols. In that case only two solvents have calculated densities less than 0.02 g/mL high, and many are more than 0.03 g/mL high. This supports the use of a 9 Å cutoff, as well as the use of the OPLS-UA parameter set.

Periodic boxes were equilibrated for a simulation time of 1 ns before data collection began. Snapshots of the dynamics of the equilibrated systems were saved every 0.3 ps for an additional 500 ps. Radial distribution functions (RDFs or $g(o\text{–}o)$) of individual snapshots were averaged over the last 500 ps of the trajectory. The RDF, also called a $g(r)$ or pair correlation function, gives the probability of a given inter-atom distance in a real fluid normalized to the probability as calculated for an ideal (i.e., unstructured) fluid, and averaged over all atoms (Allen and Tildesley, 1987; Chandler, 1987). At large separations, atoms in a real liquid no longer interact, causing the probability to be that of an unstructured fluid. The case of

interest here is the oxygen–oxygen distribution (g(o–o)), which describes the hydrogen-bonding environment of a given solvent. By integrating the RDF, the number of oxygen atoms in a certain range can be obtained:

$$n = 4\pi\rho \int_{r_1}^{r_2} g(\text{o–o}) r^2 \, dr. \tag{3}$$

Here ρ is the number of molecules per Å^3 for the specific solvent. In the case of an alcohol with a single OH group, ρ is also the density of hydroxyl groups and is proportional to 1000/molecular weight as discussed in the literature (Offeman et al., 2005b; Stephenson et al., 2006). From this integration, quantitative values are generated that represent the extended hydrogen-bonding environment, namely the average number of OH groups between 3.5 and 8.5 Å for a given solvent. The density prefactor in Eq. (3) incorporates the molecular weight, or molecular volume, into the quantification of the hydrogen-bonded networks.

A comparison of the g(o–o) function for 1-octanol using the method described here to those reported by Best et al. (1999) and Debolt and Kollman (1995) shows good agreement. Both of those studies also use the OPLS-UA forcefield, though Debolt and Kollman (1995) modify some of the torsional terms. These observations validate the use of the OPLS-UA forcefield, as well as the specific simulation settings.

3. Results and discussion

A summary of results from both molecular dynamics simulations and LLE screenings are given in Table 2 for the 54 linear and branched alcohols studied via MD simulation. It includes integrations of the g(o–o) functions for the first (0–3.5 Å), second (3.5–6 Å) and third (6–8.5 Å) solvation shells, as well as the integration for the range from 3.5–8.5 Å, the total number of carbons, the ethanol capacity (K_{DE}), and the water capacity (K_{DW}). The three regions of interest in the g(o–o), also called the solvation shells, were introduced in Stephenson et al. (2006).

Discussion of the RDFs and molecular dynamics results will examine effects of branching patterns, OH group location and molecular weight on the hydrogen-bond networks within the neat solvent. The next step is to correlate the MD results to experimental values for K_{DE} and K_{DW}.

3.1. Molecular dynamics results

As seen in Table 2, the first solvation shell integration (0–3.5 Å) is similar for all of the alcohols having 12 carbon atoms or fewer. Among these alcohols the average coordination number is 1.98 ± 0.06. Each hydroxyl group acts, on average, as a single donor and a single acceptor of hydrogen bonding. By contrast, for C > 12, the coordination numbers for the first solvation shell are much lower, ranging from 1.36 to 1.83 (i.e., each OH group has, on average, interaction with fewer than two OH groups at a time). It certainly makes since that this lowered coordination number is due to the large hydropho-

bic areas surrounding each OH group arising either from the low OH concentration or from steric hindrance caused by the high level of carbon chain branching. One would expect that as branching and steric hindrance effects increase, the ability of the hydroxyl groups to be close enough to hydrogen bond decrease and these coordination numbers also decreases. It is possible, however, that the low coordination numbers for the C16–C20 alcohols are an artifact of the OPLS-UA forcefield. The fact that calculated densities for these solvents were higher than experimental densities at least suggests that more work should be done on the C18–C20 alcohols in order to definitively separate out real intermolecular interactions from artifacts of the forcefield.

Recently, we presented MD results describing the effect of hydroxyl group location and MW on bulk liquid structure of linear alcohols ranging from C5 to C12. RDFs and trajectory snapshots were described for the x-octanol and x-decanol series ($x = 1$–4) (Stephenson et al., 2006). However, complicated branching patterns were not studied. One of the main points of interest here is to determine how isomeric variations affect the bulk liquid structure of a solvent. To do this, MD results from a subset of branched C8 alcohols were examined in detail. There were 11 C8 alcohols, which were studied by both MD and LLE. Ten of these are true isomers, and 2-ethylcyclohexanol was included even though it has two fewer H atoms. Table 3 provides the structures of these 11 alcohols organized in order of decreasing number of OH groups between 3.5 and 8.5 Å, as determined by integrating the RDFs. The trend is that the more branched an alcohol is, or the more centrally located the hydroxyl group, the smaller its extended H-bond network.

3.2. Radial distribution functions

RDFs for the o–o distributions in these alcohols are shown in Fig. 1A–C, and the corresponding integrations are plotted in Fig. 2A–C. The g(o–o) functions, and integrations, for 1-octanol through 4-octanol have already been presented (Stephenson et al., 2006), but they are repeated here for comparison with other branching patterns. Figs. 1A and 2A are the results for 1-octanol, 2-octanol, 3-octanol and 6-methyl-2-heptanol. Figs. 1B and 2B show 4-octanol, 2-methyl-4-heptanol, 4-methyl-4-heptanol and 2,2-dimethyl-3-hexanol, which are the four C8 alcohols having the smallest extended H-bond network. Figs. 1C and 2C show 2-propyl-1-hexanol, 2-ethyl-1-hexanol and the racemic mixture of 2-ethylcyclohexanol. The dashed vertical lines are located at radii of 3.5, 6 and 8.5 Å to highlight the three main regions of interest. The horizontal arrows in Fig. 2 point to the coordination number of the first solvation shell, i.e., how many other O atoms are within 3.5 Å of the central one. There are only small differences in the coordination number between all of these isomers. The largest deviations are for the highly branched and tertiary alcohols. These have first shell coordination numbers of 1.86 and 2.07 for 2,2-dimethyl-3-hexanol and 4-methyl-4-heptanol, respectively, compared to the average value of 1.98 for all of the C5–C12 alcohols.
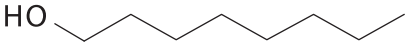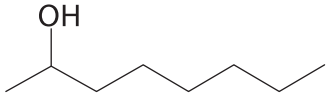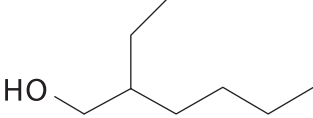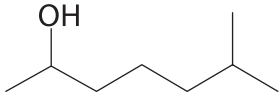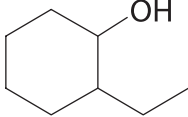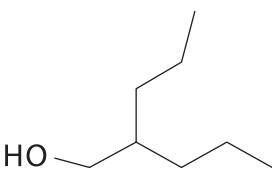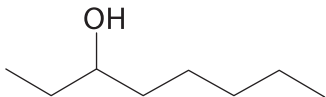
Table 2
Experimental and MD results

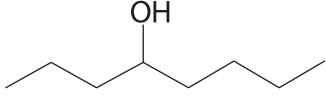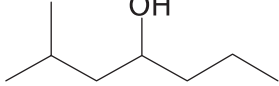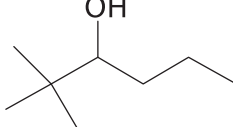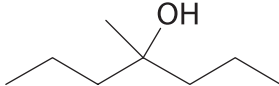| Solvent	# of carbons	Integration of g(o–o) in the range:				Liquid–Liquid extraction results	
		0–3.5 Å	3.5–6 Å	6–8.5 Å	3.5–8.5 Å	K_{DE}[a]	K_{DW}[a]
3-Pentanol[b]	5	1.91	2.27	6.58	8.86	1.29	0.105
2-Methyl-1-butanol	5	1.97	3.11	6.83	9.94	1.16	0.100
3-Methyl-3-pentanol	6	2.03	0.95	5.52	6.47	1.21	0.123
2-Methyl-3-pentanol	6	1.87	1.87	4.76	6.63	1.13	0.066
2-Methyl-2-pentanol	6	2.00	1.59	5.46	7.05	1.05	0.113
3-Hexanol[b]	6	1.92	2.28	4.92	7.20	1.06	0.062
4-Methyl-2-pentanol	6	1.99	2.40	5.21	7.61	1.02	0.078
2-Hexanol[b]	6	1.98	2.47	5.20	7.67	1.03	0.084
3,3-Dimethyl-1-butanol	6	2.01	3.15	5.54	8.69	1.08	0.081
2-Methyl-1-pentanol	6	1.94	3.06	5.76	8.82	0.92	0.067
3-Methyl-1-pentanol	6	1.98	3.26	5.68	8.94	0.93	0.079
4-Methyl-1-pentanol	6	1.99	3.48	5.74	9.22	0.95	0.083
2-Methyl-3-hexanol	7	1.90	1.73	3.40	5.13	0.80	0.041
2,4-Dimethyl-3-pentanol	7	1.90	1.28	3.91	5.19	0.85	0.045
2,2-Dimethyl-3-pentanol	7	1.96	0.98	4.37	5.35	0.81	0.040
2-Methyl-2-hexanol	7	2.10	1.38	4.37	5.75	0.97	0.080
3-Ethyl-3-pentanol	7	1.83	0.58	5.26	5.84	0.99	0.073
4-Heptanol[b]	7	1.97	2.25	3.73	5.98	0.76	0.038
3-Heptanol[b]	7	1.96	2.29	4.02	6.31	0.86	0.045
2-Heptanol[b]	7	2.01	2.37	4.44	6.81	0.86	0.064
1-Heptanol[b]	7	2.01	3.58	5.61	9.19	0.88	0.071
4-Methyl-4-heptanol	8	2.07	0.83	3.04	3.87	0.68	0.041
2,2-Dimethyl-3-hexanol	8	1.86	0.93	3.34	4.27	0.62	0.026
2-Methyl-4-heptanol	8	1.95	1.48	3.00	4.48	0.61	0.027
4-Octanol[b]	8	1.99	1.83	2.66	4.49	0.64	0.028
3-Octanol[b]	8	1.95	1.92	3.24	5.16	0.74	0.034
2-Propyl-1-pentanol	8	2.05	2.40	3.17	5.57	0.61	0.033
6-Methyl-2-heptanol	8	2.02	2.27	4.23	6.50	0.72	0.049
2-Ethyl-1-hexanol	8	2.02	2.76	4.09	6.85	0.69	0.035
2-Ethylcyclohexanol (racemic)	9	2	2.37	4.01	6.38	0.67	0.044
2-Ethylcyclohexanol (trans-)	9	1.79	2.70	4.37	7.07	N/A	N/A
2-Ethylcyclohexanol (cis-)	9	1.87	2.43	3.75	6.18	N/A	N/A
2-Octanol[b]	8	2.02	2.41	4.59	7.00	0.77	0.050
1-Octanol[b]	8	1.98	3.72	5.24	8.96	0.73	0.059
2,6-Dimethyl-4-heptanol	9	1.94	1.35	2.30	3.65	0.35	0.013
5-Nonanol[b]	9	1.98	2.00	2.76	4.76	0.54	0.022
4-Nonanol[b]	9	1.98	2.24	2.77	5.01	0.55	0.023
2-Nonanol[b]	9	2.03	2.41	3.68	6.09	0.61	0.041
1-Nonanol[b]	9	2.04	3.31	4.81	8.12	0.63	0.050
4-Propyl-4-heptanol	10	1.84	0.40	2.39	2.79	0.45	0.019
3,7-Dimethyl-3-octanol	10	1.94	0.85	2.72	3.57	0.57	0.030
4-Decanol[b]	10	1.95	1.66	2.33	3.99	0.45	0.018
3-Decanol[b]	10	1.96	1.86	3.07	4.93	0.51	0.023
2-Methyl-2-nonanol	10	1.94	1.55	3.43	4.98	0.60	0.039
2-Decanol[b]	10	2.04	2.42	3.48	5.90	0.55	0.036
1-Decanol[b]	10	2.02	3.36	4.64	8.00	0.57	0.045
5-Undecanol[b]	11	2.02	1.71	1.79	3.50	0.40	0.015
6-Undecanol[b]	11	2.03	1.80	2.04	3.84	0.40	0.014
2-Undecanol[b]	11	2.01	2.22	3.20	5.42	0.46	0.031
1-Undecanol[b]	11	2.01	3.53	4.75	8.28	0.47	0.039
2-Butyl-1-octanol	12	1.98	2.14	2.14	4.28	0.36	0.015
1-Dodecanol[b]	12	2.01	3.44	4.37	7.81	0.45	0.037
2-Hexyl-1-decanol	16	1.83	1.48	1.98	3.46	0.27	0.010
Iso-octadecanol (eight terminal CH$_3$ groups)	18	1.36	0.99	1.75	2.74	0.27	0.007
Iso-octadecanol (four terminal CH$_3$ groups)	18	1.57	1.41	1.73	3.14	0.25	0.008
2-Octyl-1-dodecanol	20	1.83	1.17	1.37	2.54	0.21	0.007

[a]Liquid–liquid extraction results from Offeman et al. (2005b, 2006).
[b]Molecular dynamics results for these alcohols were initially reported in Stephenson et al. (2006).

Table 3
Alcohol isomers containing eight carbon atoms

Name	Structure	Class	# of OH groups (3.5–8.5 Å)
1-Octanol		UP	8.96
2-Octanol		Sec	7.00
2-Ethyl-1-hexanol		BP	6.85
6-Methyl-2-heptanol		Sec	6.50
2-Ethylcyclohexanol (*cis/trans*/racemic mixture)		Sec	Racemic: 6.38 *Trans*-: 7.07 *Cis*-: 6.18
2-Propyl-1-pentanol		BP	5.57
3-Octanol		Sec	5.16
4-Octanol		Sec	4.49
2-Methyl-4-heptanol		Sec	4.48
2,2-Dimethyl-3-hexanol		Sec	4.27
4-Methyl-4-heptanol		Ter	3.87

There are several interesting observations about the g(o–o) functions (Fig. 1) and integrations (Fig. 2). First, the RDFs for 6-methyl-2-heptanol and 2-octanol (Fig. 1A) are very similar over their entire range. Integrating (Fig. 2A) all the way to a radius of 8.5 Å, shows 6-methyl-2-heptanol has only 0.5 fewer OH groups (∼ 5.5% fewer) present than 2-octanol does in the same range. The branching point for 6-methyl-2-heptanol is on the fifth carbon away from the hydroxyl group and does not af-
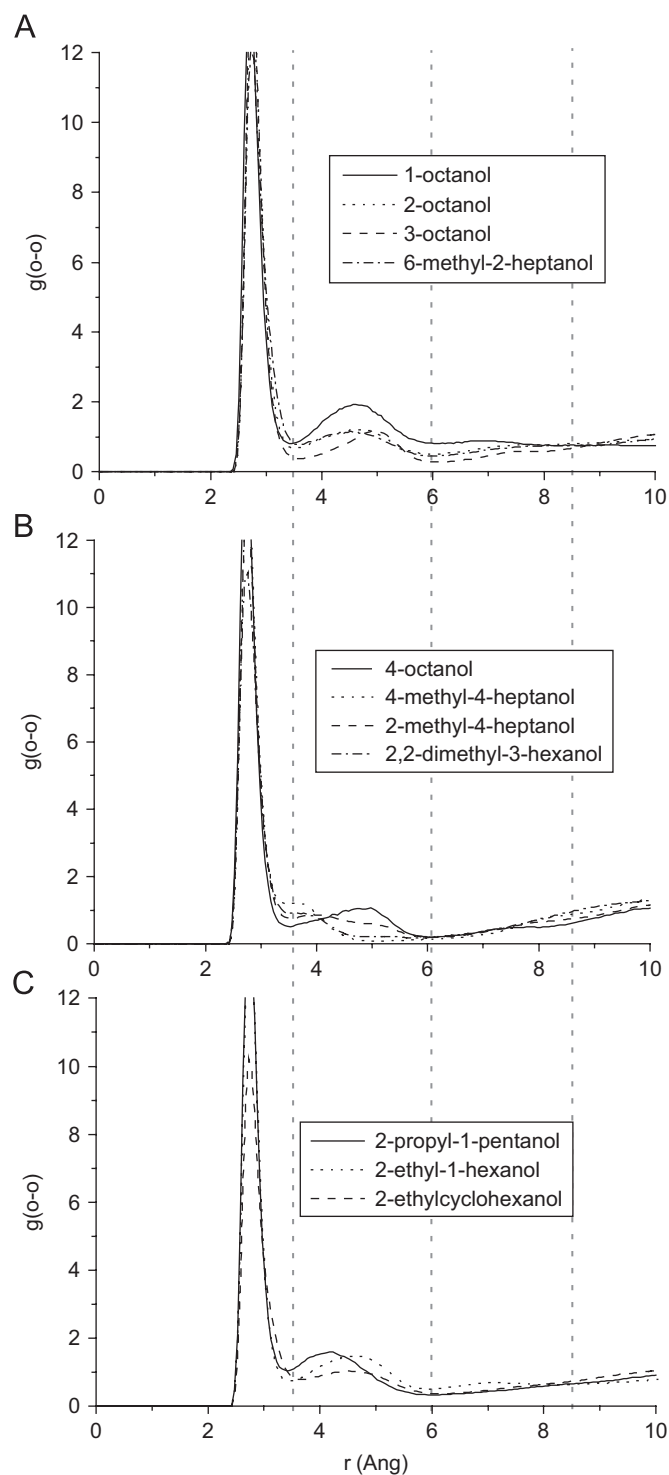
Fig. 1. RDFs for C8 alcohol isomers. (A) For 1-octanol, 2-octanol, 3-octanol and 6-methyl-2-heptanol. (B) For 4-octanol, 4-methyl-4-heptanol, 2-methyl-4-heptanol and 2,2-dimethyl-3-hexanol. (C) 2-Propyl-1-pentanol, 2-ethyl-1-hexanol and 2-ethylcyclohexanol. The vertical dashed lines designated the first, second and third solvation shells.
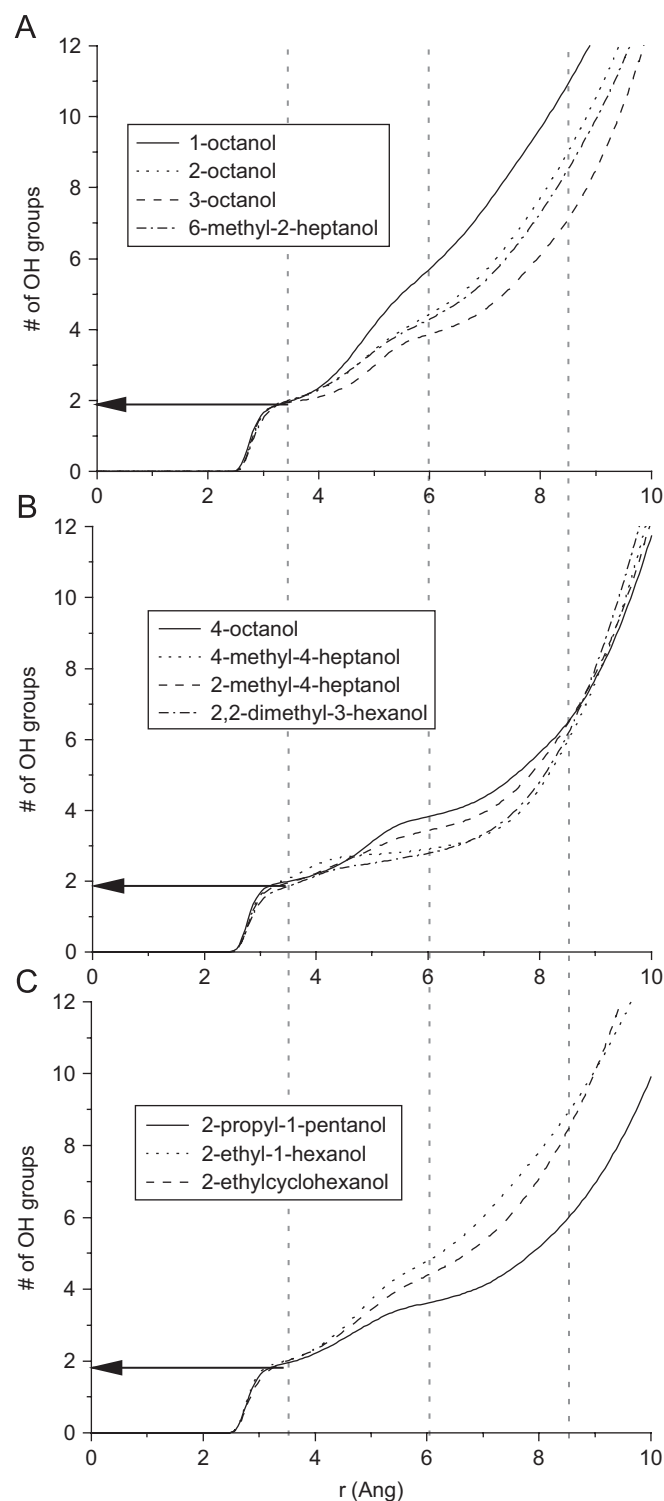
Fig. 2. Comparison of integrations of C8 alcohol isomers. (A) 1-Octanol, 2-octanol, 3-octanol and 6-methyl-2-heptanol. (B) 4-Octanol, 4-methyl-4-heptanol, 2-methyl-4-heptanol and 2,2-dimethyl-3-hexanol. (C) 2-Propyl-1-pentanol, 2-ethyl-1-hexanol and 2-ethylcyclohexanol. The vertical dashed lines designate the first, second and third solvation shells. The horizontal arrow indicates the number of OH groups corresponding to the first coordination shell.

fect the hydrogen-bonding capabilities. This supports assumptions made by Offeman et al. (2005a,b) regarding the similarities of extraction performance for alcohols with branching points removed from the OH group location.

The second set of observations deal with results plotted in Figs. 1B and Fig. 2B comparing 4-alcohols. As previously stated, 4-octanol does not have as large an extended H-bond
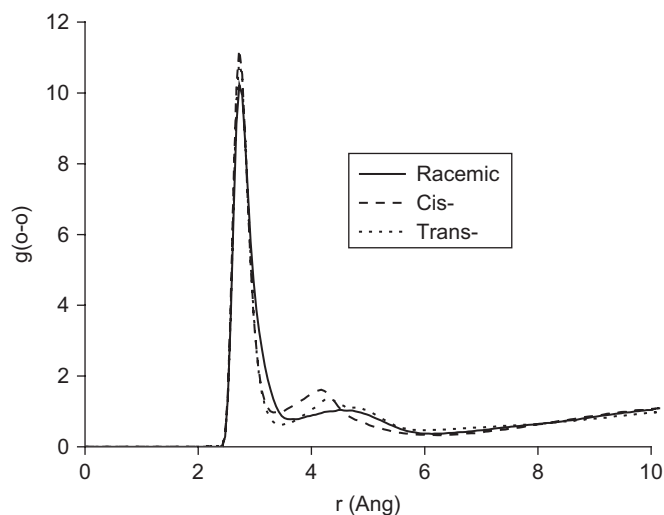
Fig. 3. RDFs for *trans-*, *cis-* and a racemic mixture of 2-ethylcyclohexanol.

network as do 1-octanol, 2-octanol and 3-octanol (Stephenson et al., 2006), and here the extended H-bond network is seen to further decrease with increased branching near the hydroxyl group. For example, 2-methyl-4-heptanol has a methyl group branch on the third carbon away from the hydroxyl group. This causes a relatively large decrease (from 1.83 to 1.48) in the integration of the second solvation shell (3.5–6 Å) as compared to 4-octanol. Moving the branching point one carbon closer to the OH group (2,2-dimethyl-3-hexanol) decreases the integration from 3.5–6 Å to 0.93 OH groups. In this case, there is also an increase in the extent of carbon chain branching compared to either 2-methyl-4-heptanol or 4-methyl-4-heptanol, which is likely also affecting the extent of hydrogen bonding. When the branching point is located on the same carbon as the hydroxyl group, as in 4-methyl-4-heptanol, the second solvation shell contains only 0.83 OH groups. Location of the carbon chain branching point closer to the OH group may interfere with the formation of large extended hydrogen-bond networks. The fact that the second solvation shell of 2,2-dimethyl-3-hexanol is more similar to 4-methyl-4-heptanol than to 2-methyl-4-heptanol could also indicate that the extent of branching makes a difference. This will be discussed in more detail in the context of Fig. 5.

The third set of observations correspond to Figs. 1C and 2C, where RDFs for the *β*-branched C8 alcohols and a ring-structured C8 alcohol are presented. Since 2-propyl-1-pentanol and 2-ethyl-1-hexanol are analogous to a 4-alcohol and a 3-alcohol, respectively, it is not surprising that the extent of the H-bond network is smaller for 2-propyl-1-pentanol than 2-ethyl-1-hexanol.

3.3. Cis- and Trans-effects

The comparison between 2-ethyl-1-hexanol and 2-ethylcyclohexanol is interesting. The periodic box for 2-ethylcyclohexanol was created with a 50:50 mixture of *cis-* and *trans-*molecules, which is the same mixture used for
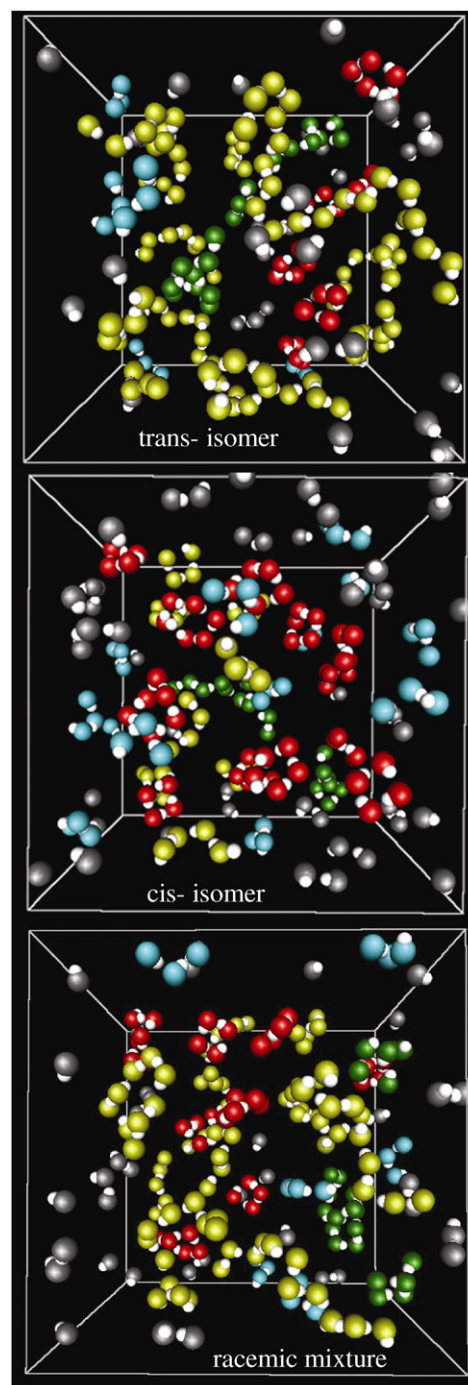

Fig. 4. Snapshots of *trans-*, *cis-* and a racemic mixture of 2-ethylcyclohexanol. Only OH groups are shown and O atoms are color-coded depending on their connectivity, via hydrogen bonding, to surrounding molecules. Straight-chains are yellow; branched chains are green; rings are red, and groups of three O-atoms are blue.

experimental solvent screening studies (Offeman et al., 2005b). Both 2-ethyl-1-hexanol and 2-ethylcyclohexanol have an ethyl group located on the *β*-carbon, but the cyclohexanol ring is confined to only a small subset of conformations, whereas the six-carbon chain on 2-ethyl-1-hexanol can rotate freely. The observation from Fig. 2C is that between
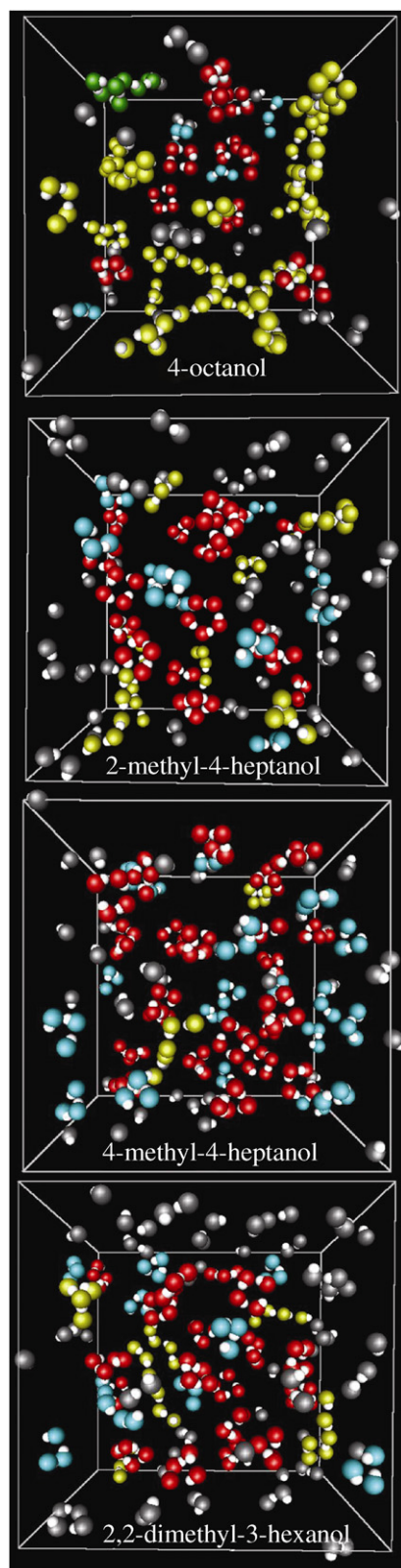
Fig. 5. Snapshots of 4-octanol, 2-methyl-4-heptanol, 4-methyl-4-heptanol and 2,2-dimethyl-3-hexanol. The color scheme is the same as that used in Fig. 4.

0 and 8.5 Å the 2-ethyl-1-hexanol and 2-ethylcyclohexanol integrations reach to 8.87 and 8.38, respectively. This is a 5.5% decrease.

Although the hexanol chain is free to rotate in 2-ethyl-1-hexanol, it is not entropically favorable for the free end to force itself near to the hydroxyl group and shield it, whereas the hexanol chain in cyclohexanol is "locked" into a position that limits OH group accessibility. The other factor here is the ethyl group orientation with regards to the hydroxyl group. For 2-ethylcyclohexanol, half of the molecules are *cis-*, so the ethyl branch is forced to remain close to the hydroxyl group. This implies that there should be more ring type structures and less hydrogen bonding. In contrast, for the *trans-* conformer, the ethyl group is permanently fixed opposite to the OH group, and this may counter-balance the effects of the *cis-*conformer.

Simulations on periodic boxes containing 100% *trans-* and 100% *cis-*2-ethylcyclohexanol result in $g(\text{o–o})$ functions for the *cis-*system that differ from the *trans-* and racemic systems primarily in the second solvation shell. The RDF for the *trans-* simulation is nearly the same as for the racemic mixture with the differences being a narrowing in the first solvation shell and a slight increase in the amplitude of the peak in the second solvation shell (Fig. 3). When the integrations are compared, the average numbers of OH groups from 3.5 to 8.5 Å are 6.18 and 7.07 for the *cis-* and *trans-*isomers, respectively. This result for the racemic mixture is 6.38, which is between that of the individual species. Although the RDFs for these three systems are relatively similar, snapshots from each of these trajectories are strikingly different as shown in Fig. 4. All carbon atoms are masked, and O atoms are color-coded depending on the hydrogen-bonding in which they participate. The snapshot for the *trans-*isomer has many more long chains and branches than the *cis-*isomer, which contains primarily hydroxyl group rings and groups of three. When the ethyl group is on the same side of the ring as the OH group, it hinders the formation of long-extended hydrogen-bonded structures. The snapshot for the racemic mixture is somewhere between the *cis-* and *trans-* isomers as far as composition of chains, branches, rings and groups of three. The location and orientation of branches on the carbon chain near the OH group affects the interactions that occur between solvent molecules.

3.4. Liquid structure snapshots

Snapshots from the trajectories calculated for 4-octanol, 2-methyl-4-heptanol, 4-methyl-4-heptanol and 2,2-dimethyl-3-hexanol (Fig. 5) provide an additional view of the H-bond network. The color-coding is the same as used in for Fig. 4. As the branching point is located closer to the OH-group, the fewer straight-chain or branched chain H-bond networks are present. These larger structures split into many ring structures containing 4–5 hydroxyl groups as well as small clusters of 3 OH groups. The main differences between 2-methyl-4-heptanol and 4-methyl-4-heptanol are the decreased number of straight-chains and the increase in "clusters" containing just three OH groups. The snapshot for 2,2-dimethyl-3-hexanol has more straight-chains, fewer rings and fewer groups of three, but more isolated dimer-like groups than 4-methyl-4-heptanol. Despite similar $g(\text{o–o})$ functions and integrations, there are

differences between these two snapshots. Since the RDFs are averages over every O atom in a snapshot, the influence of having more chain structures, with $\geqslant 4$ OH groups, is balanced by the increased number of dimer structures and the subsequent decrease in numbers of rings and three O atom groups.

That the hydrogen-bonded structure within an alcohol is highly dependent on the specifics of its molecular structure is not surprising due to steric effects and accessibility of the hydroxyl group. The comparison with this series of C8 alcohols provides some sense of the extent to which different structural modifications alter the bulk hydrogen-bonding ability of the solvent. For example, having a methyl branch on the fifth carbon from the OH group changes the observed RDF only minimally (2-octanol vs. 6-methyl-2-heptanol), but locating the methyl group on the 2- vs. the 4-position of 4-heptanol causes a large morphological change in the RDF (2-methyl-4-heptanol vs. 4-methyl-4-heptanol). Orientation differences in locations of branches near to, or away from, the OH group also affect the hydrogen-bonding characteristics, as for *cis-* and *trans-*2-ethylcyclohexanol.

In summary, a centrally located hydroxyl group, carbon chain branching and the location of the branch near the hydroxyl group are all factors that interrupt the formation of extended hydrogen-bond networks and cause hydroxyl groups to form multiple small groups, or ring structures, rather than long winding chains.

3.5. Extraction correlation

At this point the question naturally arises as to whether these MD results can explain the ethanol and water capacity trends observed for the various solvents, or perhaps be used as a tool to predict LLE results. In Stephenson et al. (2006), the response to this was based on results for only the primary and secondary linear alcohols. However, when branched alcohols are examined, correlation is no longer as clear. Adding results from various branching patterns on both primary and secondary alcohols and including tertiary alcohols highlights perturbing differences in trends between the extended H-bond network (3.5–8.5 Å) and K_{DW}, or K_{DE}, for different classes of alcohols. It should be noted that in all of these cases, error bars are not included for the experiment K_{DW} and K_{DE} values as these are quite small. More details on the experimental methods used to determine ethanol and water capacities are included in Offeman et al. (2005a).

The updated correlation is shown in Fig. 6A and B for experimental K_{DE} and K_{DW} values, respectively. Four classes of alcohols are distinguished as unbranched primary (UP), branched primary (BP), secondary (Sec) or tertiary (Ter). The one ring containing alcohol, a racemic mixture of 2-ethylcyclohexanol, is grouped with the secondary alcohols. Least-squares fits were performed on the data and their corresponding R^2 values are listed. Linear fits were done on the UP series, and all other series were fit using an exponential function. As with the purely linear primary and secondary alcohols (Stephenson et al., 2006), correlation of the H-bond network to K_{DW} is generally better
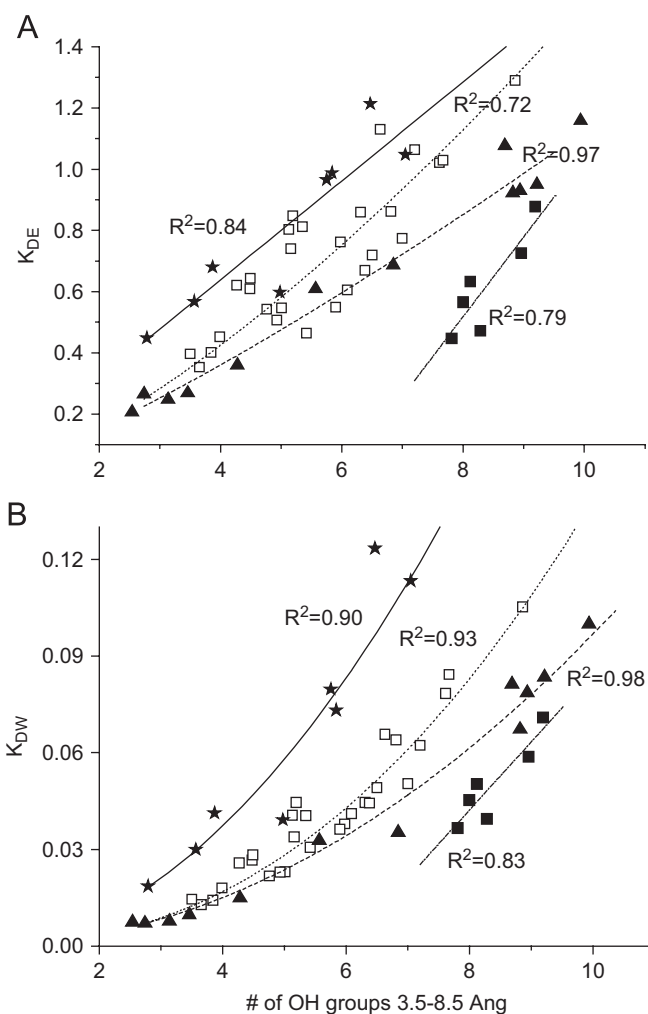

Fig. 6. Number of OH 3.5–8.5 vs. K_{DE} and K_{DW}. These are attempted correlations between results from MD simulations and experimental liquid–liquid extraction results. The different classes of alcohols are represented by: ■, unbranched primary (UP); ▲, branched primary (BP); □, secondary (Sec); and ⋆, tertiary (Ter). Least-squares fits are included with their corresponding R^2 values. (A) shows these correlations with K_{DE}, and (B) shows them for K_{DW}.

than to K_{DE}, especially for the secondary alcohols. The exception is the BP class, for which K_{DE} and K_{DW} fit equivalently. It should also be noted that the correlations for K_{DE} in Fig. 6A are not as good as that between 1000/MW and K_{DE} across all data points ($R^2 = 0.93$) (Offeman et al., 2005b, 2006).

There are two reasonable alternatives to using the number of OH groups between 3.5 and 8.5 Å to quantify the extended H-bond network. A case can be made for the use of either the second (3.5–6 Å) or the third (6–8.5 Å) solvation shell separately. The RDFs show the most dramatic differences in the second solvation shell, but longer-range correlations (third shell) may be more relevant to the issue of a solvent's capacity for either ethanol or water. Fig. 7A and B show correlations of the second solvation shell to K_{DE} and K_{DW}, respectively. The extent of scatter in these plots makes attempts at fitting them futile. Although the general observation that UP alcohols have the most
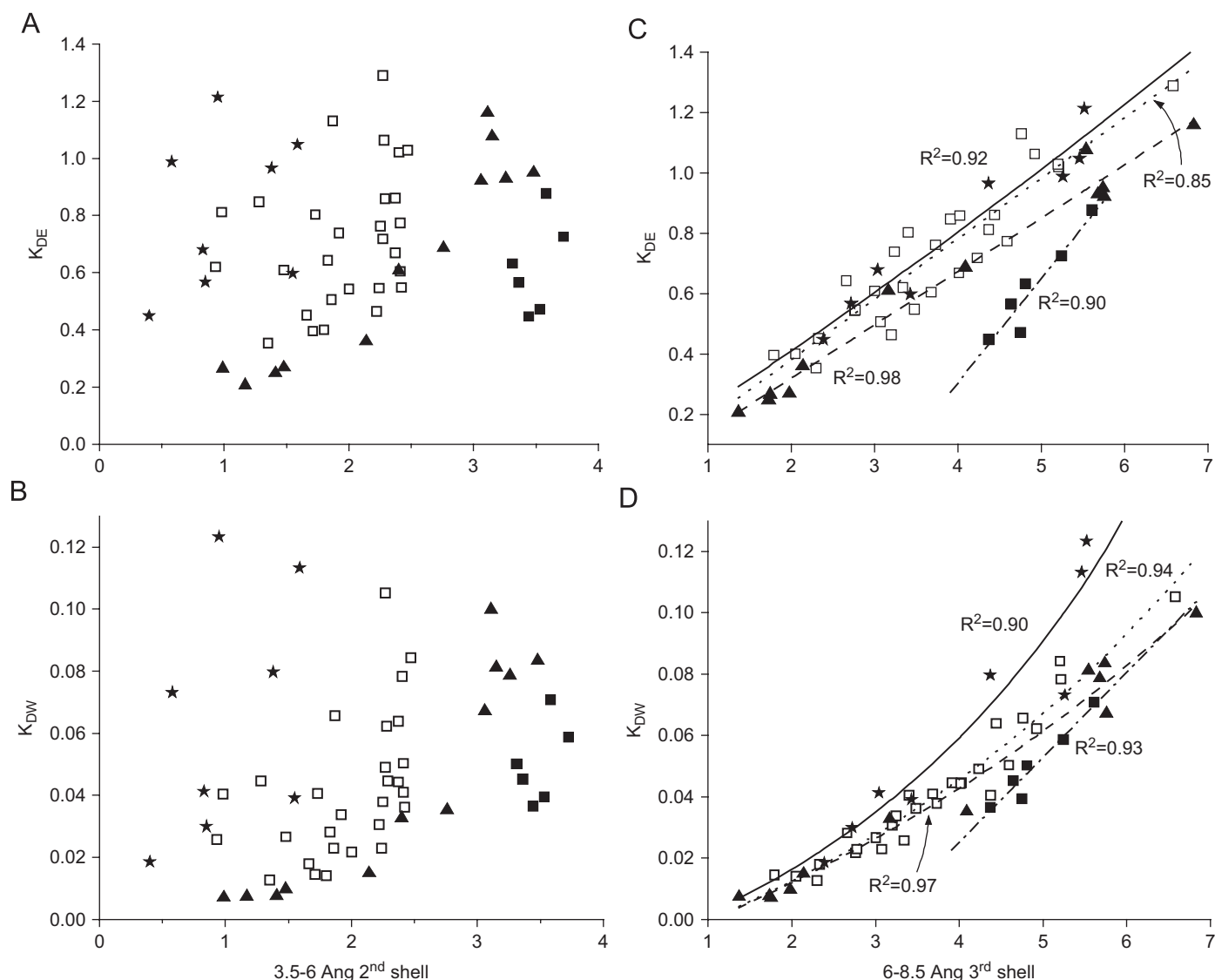
Fig. 7. Number of OH groups in the 3.5–6 and 6–8.5 Å ranges correlated to K_{DW} and K_{DE}. Classes of alcohols are represented by: ■, unbranched primary (UP); ▲ branched primary (BP); □, secondary (Sec); and ★ tertiary (Ter). (A) and (B) correlate the second solvation shell (3.5–6 Å) with K_{DE} and K_{DW}, respectively. (C) and (D) correlate the third solvation shell (6–8.5 Å) with K_{DE} and K_{DW}, respectively. Least-squares fits are included for the correlations of the third solvation shell.

OH groups between 3.5 and 6 Å, followed, in decreasing order, by the BP, secondary and tertiary alcohols holds true for both K_{DE} and K_{DW}. Correlations, including least-squares fits and R^2 values, for the third solvation shell to K_{DE} and K_{DW} are given in Fig. 7C and D. For K_{DW} these fits are the same as when correlated to the number of OH groups between 3.5 and 8.5 Å, except in the case of the UP alcohols, which are fit slightly better in Fig. 7D. For K_{DE} correlating to only the third solvation shell improves the fits for all groups of alcohols. The interactions in the third solvation shell are more similar to the bulk properties of a given solvent, and therefore, to the OH group concentration, another way of viewing 1000/MW.

As previously mentioned the H-bond network is being used as a single value, or parameter which accounts for multiple char-

acteristics of the solvent, namely molecular weight, hydroxyl position and branching patterns. One illustration of the shortcomings of using the extended H-bond network to correlate to with the solvent's water capacity is shown in Fig. 8. This is for the case of the H-bond network from 3.5 to 8.5 Å against K_{DW} for the 11 C8 alcohols discussed earlier. As shown in Fig. 8, the H-bond network to K_{DW} plot shows a nice correlation for all but two of the alcohols tested. 4-Methyl-4-heptanol and 2-ethyl-1-hexanol fall outside of the trend set by the other nine C8 alcohols. It is unclear why this is the case.

For example, if the capacity for water is simply dependent on the accessibility of the hydroxyl groups in the solvent, as proposed by Stephenson et al. (2006), then it does not follow that 4-methyl-4-heptanol, which has a RDF similar to 2,2-dimethyl-
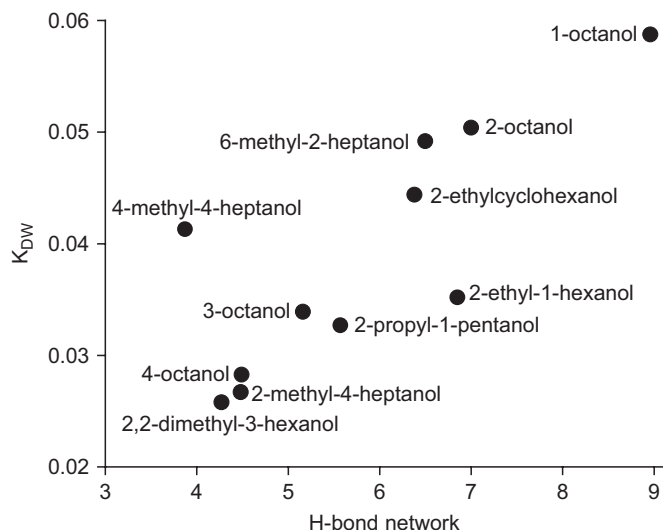
Fig. 8. Plotted and labeled here is the number of OH groups between 3.5 and 8.5 Å vs. water capacity for the eight carbon isomers.

3-hexanol, has a 35% higher K_{DW}. Furthermore, if the presence of small OH group rings surrounded by a hydrophobic layer is the sole cause of the decreasing K_{DW}, then the fact that 4-methyl-4-heptanol, which has the most small ring structures of any of the C8 alcohols, has a higher K_{DW} than six of the solvents with larger extended H-bond networks is inconsistent. In fact, the different trends in Figs. 6 and 7 for UP, BP, secondary and tertiary alcohols have already suggested that something beyond mere neat liquid structure is affecting the water capacities. Additionally, both water and ethanol are present in the solvent and the interactions between each of those and the solvent, as well as with each other, could explain why the pure solvent hydrogen-bonded network does not correlate perfectly with experimental extraction results.

4. Conclusions

Direct correlation between the extended hydrogen-bonded network in alcohols and experimental LLE results works for primary and secondary unbranched alcohols, but not for data that includes branched alcohols. However, these molecular dynamics results still provide a useful molecular-level snapshot of the interactions occurring within the alcohols which qualitatively enhances the understanding of these systems. The use of molecular dynamics simulation results provides a method of combining solvent structure (i.e., molecular weight, hydroxyl position and branching patterns) and intermolecular interactions (i.e., hydrophobic and van der Waals interactions) into a single parameter, which helps correlate extraction performance.

Experimental determination of RDFs via neutron diffraction for a subset of these alcohols would be useful to validate the results obtained by molecular dynamics, especially for the C18–C20 alcohols. Also, extending the molecular dynamics simulations to mixtures of solvent, ethanol and/or water might resolve apparent branched alcohol anomalies.

The approach described here provides interesting insights into the liquid structure and functional character of neat alcohols. Surprisingly little information is available in the literature regarding the hydrogen-bonding characteristics of alcohols containing 5–20 carbon atoms or the effects of complicated branching patterns on their RDFs. Progress has been made here in observing the qualitative effects of factors such as branching location on the hydrogen-bonded network. Comparing the RDFs and snapshots of OH group configurations for series of alcohols provide insight into molecular-level "structures" and interactions within these systems.

References

Allen, M.P., Tildesley, D.J., 1987. Computer Simulation of Liquids. University Press, New York, pp. 54–58, 90–98 and 156–162.

Bakó, I., Jedlovsky, P., Pálinkás, G., 2000. Molecular clusters in liquid methanol: a reverse Monte Carlo study. Journal of Molecular Liquids 87, 243–254.

Berendsen, H.J.C., Postman, J.P.M., van Gunsteren, W.F., DiNola, A., Haak, J.R., 1984. Molecular dynamics with coupling to an external bath. Journal of Chemical Physics 81, 3684–3690.

Best, S.A., Merz Jr., K.M., Reynolds, C.H., 1999. Free energy perturbation study of octanol/water partition coefficients: comparison with continuum GB/SA calculations. Journal of Physical Chemistry B 103, 714–726.

Bowron, D.T., Moreno, S.D., 2002. The structure of a concentrated aqueous solution of tertiary butanol: water pockets and resulting perturbations. Journal of Chemical Physics 117, 3753–3762.

Bowron, D.T., Moreno, S.D., 2003. Structural correlations of water molecules in a concentrated alcohol solution. Journal of Physics: Condensed Matter 15, S121–S127.

Bowron, D.T., Finney, J.L., Soper, A.K., 1998. The structure of pure tertiary butanol. Molecular Physics 93, 531–543.

Chandler, D., 1987. Introduction to Modern Statistical Mechanics. Oxford University Press, New York, pp. 195–218

Chen, B., Potoff, J.J., Siepmann, J.I., 2001. Monte Carlo calculations for alcohols and their mixtures with alkanes. Transferable potentials for phase equilibria. 5. United-atom description of primary, secondary, and tertiary alcohols. Journal of Physical Chemistry B 105, 3093–3104.

Chen, C.C., Mathias, P.M., 2002. Applied thermodynamics for process modeling. A.I.Ch.E. Journal 48, 194–200.

Daugulis, A.J., Axford, D.B., McLellan, P.J., 1991. The economics of ethanol production by extractive fermentation. Canadian Journal of Chemical Engineering 69, 488–497.

Debolt, S.E., Kollman, P.A., 1995. Investigation of structure, dynamics, and solvation in 1-octanol and its water-saturated solution: molecular dynamics and free-energy perturbation studies. Journal of the American Chemical Society 117, 5316–5340.

Dixit, S., Crain, J., Poon, W.C.K., Finney, J.L., Soper, A.K., 2002. Molecular segregation observed in a concentrated alcohol–water solution. Nature 416, 829–832.

Eckert, F., Klamt, A., 2002. Fast solvent screening via quantum chemistry: COSMO-RS approach. A.I.Ch.E. Journal 48, 369–385.

Fredenslund, A., Jones, R.L., Prausnitz, J.M., 1975. Group-contribution estimation of activity coefficients in nonideal liquid mixtures. A.I.Ch.E. Journal 21, 1086–1099.

González, M.A., Bermejo, F.J., Enciso, E., Cabrillo, C., 2004. Hydrogen bonding in condensed-phase alcohols: some keys to understanding their structure and dynamics. Philosophical Magazine 84, 1599–1607.

Jorgensen, W.L., 1986. Optimized intermolecular potential functions for liquid alcohols. Journal of Physical Chemistry 90, 1276–1284.

Kim, S., Dale, B.E., 2004. Global potential bioethanol production from wasted crops and crop residues. Biomass and Bioenergy 26, 361–375.

King, C.J., 1971. Separation Processes. McGraw-Hill Book Company, San Francisco, pp. 23–40

Klamt, A., 2005. Cosmo-RS From Quantum Chemistry to Fluid Phase Thermodynamics and Drug Design. Elsevier, Amsterdam.

Laaksonen, A., Kusalik, P.G., Svishchev, I.M., 1997. Three-dimensional structure in water–methanol mixtures. Journal of Physical Chemistry A 33, 5910–5918.

Lynd, L.R., Wyman, C.E., Gerngross, T.U., 1999. Biocommodity engineering. Biotechnology Progress 15, 777–793.

Madson, P.W., Monceaux, D.A., 1999. Fuel ethanol production. In: Jacques, K.A., Lyons, T.P., Kelsall, D.R. (Eds.), The Alcohol Textbook. A Reference for the Beverage, Fuel and Industrial Alcohol Industries, third ed. Nottingham University Press, Nottingham, UK, pp. 257–268.

Magnussen, T., Resmussen, P., Fredenslund, A., 1981. UNIFAC parameter table for prediction of liquid–liquid equilibriums. Industrial and Engineering Chemistry Process Design and Development 20, 331–339.

Maiorella, B.L., Blanch, H.W., Wilke, C.R., 1984. Economic evaluation of alternative ethanol fermentation processes. Biotechnology and Bioenergy 26, 1003–1025.

Munson, C.L., King, C.J., 1984. Factors influencing solvent selection for extraction of ethanol from aqueous solutions. Industrial and Engineering Chemistry Process Design and Development 23, 109–115.

Offeman, R.D., Stephenson, S.K., Robertson, G.H., Orts, W.J., 2005a. Solvent extraction of ethanol from aqueous solutions. I. Screening methodology for solvents. Industrial and Engineering Chemistry Research 44, 6789–6796.

Offeman, R.D., Stephenson, S.K., Robertson, G.H., Orts, W.J., 2005b. Solvent extraction of ethanol from aqueous solutions. II. Linear, branched, and ring-containing alcohol solvents. Industrial and Engineering Chemistry Research 44, 6797–6803.

Offeman, R.D., Stephenson, S.K., Robertson, G.H., Orts, W.J., 2006. Solvent extraction of ethanol from aqueous solutions using biobased oils, alcohols and esters. Journal of the American Oil Chemists Society 83, 153–157.

Othmer, D.F., Ratcliffe, R.L., 1943. Alcohol and acetone by solvent extraction. Industrial and Engineering Chemistry 35, 798–805.

Padró, J.A., Saiz, L., Garcia, E., 1997. Hydrogen bonding in liquid alcohols: a computer simulation study. Journal of Molecular Structure 416, 243–248.

Poling, B.E., Prausnitz, J.M., O'Connell, J.P., 2001. The Properties of Gases and Liquids, fifth ed. McGraw-Hill, New York.

Ponder, J.W., 2004. TINKER: Software Tools for Molecular Design (4.2 edition). Washington University School of Medicine, St. Louis.

Prausnitz, J.M., Tavares, F.W., 2004. Thermodynamics of fluid-phase equilibria for standard chemical engineering operations. A.I.Ch.E. Journal 50, 739–761.

Stephenson, S.K., Offeman, R.D., Roberston, G.H., Orts, W.J., 2006. Ethanol and water capacities of alcohols: a molecular dynamics study. Chemical Engineering Science 61, 5834–5840.

Van Leeuwen, M.E., 1996. Prediction of the vapour–liquid coexistence curve of alkanols by molecular simulation. Molecular Physics 87, 87–102.

Wu, H.S., Sandler, S.I., 1991. Use of ab initio quantum mechanics calculations in group contribution methods. 1. Theory and the basis for group indentifications. Industrial and Engineering Chemistry Research 30, 881–889.

Wyman, C.E., 2003. Potential synergies and challenges in refining cellulosic biomass to fuels, chemicals and power. Biotechnology Progress 19, 254–262.